THE JOURNAL OF PHYSICAL CHEMISTRY B LETTERS

2006, *110,* 14035−14039
Published on Web 06/30/2006

A Full Multiple Scattering Model for the Analysis of Time-Resolved X-ray Difference Absorption Spectra

Maurizio Benfatto,[†] Stefano Della Longa,[†,‡] Keisuke Hatada,[†] Kuniko Hayakawa,[†] Wojciech Gawelda,[§] Christian Bressler,[§] and Majed Chergui*[,§]

Laboratori Nazionali di Frascati, INFN, CP13, I-00044 Frascati, Italy, Dipartimento di Medicina Sperimentale, Universitá dell'Aquila, 67100 L'Aquila, Italy, and Laboratoire de Spectroscopie Ultrarapide (LSU), ISIC-FSB, BSP, Ecole Polytechnique Fédérale de Lausanne (EPFL), CH-1015 Lausanne-Dorigny, Switzerland

Received: May 30, 2006; In Final Form: June 16, 2006

A full multiple theoretical model (MXAN) is applied to fit picosecond difference X-ray absorption spectra at the ruthenium L_3 edge upon photoexcitation of aqueous $[Ru^{II}(bpy)_3]^{2+}$. We show that fitting difference spectra allows an increase in sensitivity, such that slight structural changes can be retrieved, which are not detected in fitting full spectra. The Ru−N bond distances of the excited complex in the ^{3}MLCT state are in good agreement with recently published values. The implementation of the present approach to L-edge spectra and its high sensitivity opens opportunities for its extension to a large class of experiments where difference X-ray absorption spectra are recorded.

I. Introduction

X-ray Absorption spectroscopy (XAS) delivers details about the electronic structure of an atom of interest, i.e., orbital occupancy, degree of oxidation, and ligand field strength of its valence states, which are those driving chemical reactions, via X-ray absorption near-edge structure (XANES) spectroscopy. Simultaneously, coordination numbers and bond distances around a specific atom can be determined from the extended X-ray absorption fine structure (EXAFS) spectroscopy.

In recent years, there has been growing activity using XAS in a pump−probe scheme to detect photoinduced electronic and structural changes in real time. In these experiments, the system is excited by an ultrashort pump laser pulse and is probed by a short X-ray probe pulse, whose time delay with respect to the laser pump pulse can be continuously varied.[1] Bressler, Chergui, and co-workers[2−5] pioneered the differential transient absorption spectroscopy (XANES and EXAFS), which consists of recording the difference between the transmission spectra of the unexcited and laser-excited sample. This increases greatly the sensitivity of the experiment (differential signals below 10^{-4} optical density (OD) can be identified, thanks also to the high stability of synchrotron sources), while largely reducing systematic errors such as intensity fluctuations or deterioration of the sample during the experiment.[4,5] Recently, a variant of this approach was used in a dispersive XAS setup, to retrieve by EXAFS very small structural changes induced by magnetostriction on an iron−cobalt film.[6] These studies show the potential of differential X-ray absorption spectroscopy, not only in the case of light-induced or magnetic-field induced changes, but also when the changes are induced by temperature,[7,8] pressure,[9,10] pH changes (important in biology),[11−13] and so forth.

The importance of differential XAS for theoretical modeling can only be emphasized, as fitting difference spectra has the important advantage of increasing the sensitivity of the fit and decreasing the influence of possible systematic errors in the calculations, which come from the approximations used in the theoretical approach. In the above study by Pettifer et al.,[6] the simulations were limited solely to the differential EXAFS spectra of the Fe K edge, and there has so far not been a theoretical study of differential XANES spectra. In recent years, Benfatto and co-workers[14] have developed a fitting procedure (called MXAN) based on a full multiple scattering analysis of X-ray absorption features.[15] However, this approach has not been implemented in the case of differential spectra, let alone at L edges.

This contribution presents new extensions of MXAN, to the case of the recently published[2,16] picosecond L_3-edge XANES and EXAFS difference spectra of a coordination compound, $[Ru^{II}(bpy)_3]^{2+}$ in a water solution, excited by a 400 nm ultrashort laser pulse. This excitation brings the molecule to the singlet metal-to-ligand charge-transfer (MLCT) state, which then undergoes ultrafast (<100 fs) intersystem crossing to the low-lying ^{3}MLCT state,[17] whose radiative lifetime is on the order of several hundreds of nanoseconds. In the process, the central Ru atom is oxidized because an electron is transferred to the bpy ligands. Gawelda et al.[16] recorded the differential XAS spectra between the ground state and the excited complex in its ^{3}MLCT state, from which the excited state XAS can be reliably constructed.

The analysis of the XANES line shapes using an atomic multiplet code,[18] with both octahedral and trigonal ligand fields superimposed to describe the excited-state complex and of the EXAFS region of the excited states, pointed to a contraction of Ru−N bonds by ∼0.035 Å in the excited-state complex. However, this treatment handled the bound−bound and bound−

[†] INFN.
[‡] Universitá dell'Aquila.
[§] Ecole Polytechnique Fédérale de Lausanne.

10.1021/jp063326o CCC: $33.50

continuum transitions with different theoretical approaches. It also left an above-ionization resonance (the so-called C-feature, see below) unassigned, and the structural analysis was limited to the first shells of N and C atoms surrounding the Ru atom. Finally, it assumed a trigonal symmetry for the excited complex. While this last assumption seems justified, in part because of the excellent agreement between the simulated and experimental XANES line shapes,[16] strictly speaking, the excited complex has a C_2 symmetry.

This present contribution introduces a number of novel aspects: (i) Using MXAN, we provide a global approach for the description, in a consistent way, of the bound−bound and bound−continuum features of the spectra. (ii) We implement for the first time MXAN, to analyze L-edge spectra of metals and demonstrate its applicability to coordination chemistry compounds. (iii) We apply it to the simulation of differential spectra and show that this improves the sensitivity and thus delivers structural information about transient species, that the simulation and fit of full spectra cannot retrieve. These points underscore the importance of the present procedure to a very broad range of systems and phenomena, where XAS is used to monitor weak changes, caused by an external perturbation.

II. Theoretical Details

The quantitative analysis of the energy region around the L_3 edge of Ru was performed using the MXAN code, with the aim of deriving structural information, using the same procedure described in refs 14 and 19. The method is based on the comparison between experimental data and several theoretical calculations performed by varying selected structural parameters starting from a well-defined initial geometrical configuration around the absorber. The optimization in parameter space is achieved by minimization of the square residual function

$$R_{\mathrm{aq}} = n \frac{\sum_{i=1}^{m} w_i[(y_i^{\mathrm{th}} - y_i^{\mathrm{exp}})\epsilon_i^{-1}]^2}{\sum_{i=1}^{m} w_{\mathrm{i}}}$$

where n is the number of independent parameters, m is the number of data points, y_i^{th} and y_i^{exp} are the theoretical and experimental values of absorption, respectively, ϵ_i is the individual error in the experimental data set, and w_i is a statistical weight. For $w_i = 1$, the square residual function R_{sq} becomes the statistical χ^2 function. In this paper, we assume a constant experimental error ϵ equal to 0.6% of the main jump for the whole experimental data set.

Theoretical calculations are performed within the so-called full multiple scattering (FMS) approach, i.e., the inverse of the scattering path operator is computed exactly, avoiding any "a priori" selection of the relevant MS paths, and using the muffin-tin (MT) approximation for the shape of the potential.[15] The MT radii are chosen according to the Norman criterion with specified percentage of overlap, and the potential is recalculated at each step of the minimization procedure, keeping the overlap factor fixed.

The exchange and correlation part of the potential is calculated in the framework of the Hedin−Lundqvist (HL) scheme. To avoid overdamping of the spectrum at low energies, caused by the use of the full complex HL potential, MXAN uses a phenomenological approach to calculate the inelastic losses.[20,21] It is based on the convolution of the theoretical spectrum, calculated using only the real part of the HL potential, with a suitable Lorentzian function with an energy-dependent width given by $\Gamma = \Gamma_c + \Gamma(E)$. The constant part Γ_c accounts for contributions of the core hole lifetime and the experimental resolution, while the energy-dependent term $\Gamma(E)$ represents both intrinsic and extrinsic inelastic processes. $\Gamma(E)$ is zero below an onset energy E_s and begins to increase from a value A_s, following the universal functional form of the mean free path in a solid. This method introduces three nonstructural parameters that are derived during the fit on the basis of a Monte Carlo search, at each step of the computation. Application of this procedure to different systems confirmed the reliability of this approach.[22,23]

The fits of the XANES difference absorption spectra between excited- and ground-state Ru compounds ($Ru^{es} - Ru^{gs}$) have been obtained by a modification of the MXAN program, using the following procedure: First, the theoretical XANES spectrum of Ru^{gs} is calculated as a reference using the structural coordinates obtained by the direct fit of the ground state. This structure is equal, within the statistical errors, to the crystallographic determination. Then, MXAN calculates various theoretical spectra, one at each step of the fit, for all the different structures obtained by varying the selected coordinate parameters starting from the spectrum. All these XANES spectra have been calculated using only the real part of the HL potential, i.e., without including any damping factor. Finally, using the procedure previously described, the real theoretical difference spectrum is convoluted in order to compare with the experimental data and to reach the best-fit condition. This procedure assumes that the damping parameters are not correlated to the structural parameters and are identical for both ground and excited states. The number of nonstructural parameters used by this new procedure is equal to that fitting the full spectra.

The non-MT corrections are normally very weak and confined to the first 10−20 eV from the edge, with a very small influence on the structural determination as demonstrated in several test cases.[15−18] However, they can provide some additional details on the potential-energy landscape around the absorbing atom, due to the lifting of the muffin-tin averaging approximations. Indeed, in the MT approximation, the potential is spherically symmetric in nonoverlapping spheres defined around each atom and is assumed constant in the interatomic region. This is a drawback, in particular, in the region at very low energy, where the fine details of the potential are important, because the photoelectron energy is low and on the order of the error in the value of the potential. To assess the relevance of these non-MT corrections, we have also performed full potential calculations. These are based on the finite difference method (FDM), which is a method to solve the Schrödinger equation (SE) for a potential of general shape.[24] Essentially, it writes the SE equation over a three-dimensional grid, obtaining a very large system of linear equations connecting the value of the wave function on all of the grid points. We have used the FDMSE program developed by Joly.[25] The exchange and correlation part of the potential is again calculated by the HL scheme, using only the real part.

III. Results and Discussion

Figure 1 shows the X-ray absorption spectrum of $[Ru^{II}(bpy)_3]^{2+}$ in the region of the L_3 and L_2 edges (a), the differential absorption spectrum obtained 50 ps after laser excitation (b), and the X-ray absorption spectrum of the excited compound in the ^{3}MLCT (c) retrieved from spectra (a) and (b), using a photolysis yield of 10%, measured in laser pump−probe

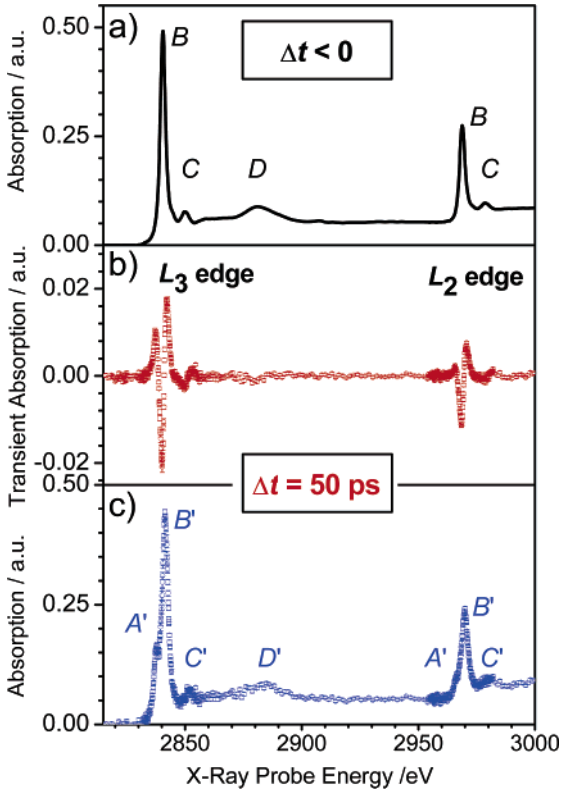

Figure 1. (a) Static absorption spectrum of aqueous $[Ru(bpy)_3]^{2+}$ in the region of the Ru L_3 and L_2 edges. (b) Transient difference absorption spectrum measured 50 ps after photoexcitation. (c) Excited-state XAS spectrum extracted from spectra a and b (see ref 16 for details). Note that, in comparison with spectrum a, an additional band (A′) shows up.

experiments (see ref 16 for details). The ground-state spectrum exhibit bands labeled B, C, and D. The B-band is assigned to transition from the 2p core shell to the ligand field split empty 4d(e_g) level (all 6 electrons of Ru^{II} are in the lowest 4d(t_{2g}) level). In ref 16, we tentatively assigned band C to an above-ionization resonance. This interpretation is confirmed by the present simulations (see below). Finally, band D is clearly an above-ionization scattering feature.[16]

In the excited complex (Figure 2), the analogues of the B, C, and D bands are all recovered (primes are used for the excited state), along with an additional one (A′), which appears below the B′ band, because we have created a hole in the previously filled t_{2g} level, as a result of the photoexcitation that transfers an electron from the Ru atom to one of the bpy ligands.

In the following analysis, we will only concentrate on the L_3 edge[16] and first fit its full spectra in the ground and excited states (Figure 1a,c). The known crystallographic data of the ground state is taken as initial structure.[26,27] This choice is reasonable, as it was found that the EXAFS spectra are well-reproduced with these input parameters.[16] The entire cluster of 37 atoms (1 Ru, 6 N, and 30 C atoms of the bpy ligands, disregarding the outermost 30 H atoms) has been used in the present analysis. The structural parameters allowed to change during the fitting procedure are as follows: (i) two distances between the absorber and the nitrogen atoms of the three rings up and down the plane perpendicular to the C_3 axis and (ii) the angle of one triplet with respect to the other two. The atoms of each ring are linked to the corresponding nitrogen and move with it during the fit. Rings up and down are linked during the movement; in this way, only three independent structural parameters are used in the fit procedure.

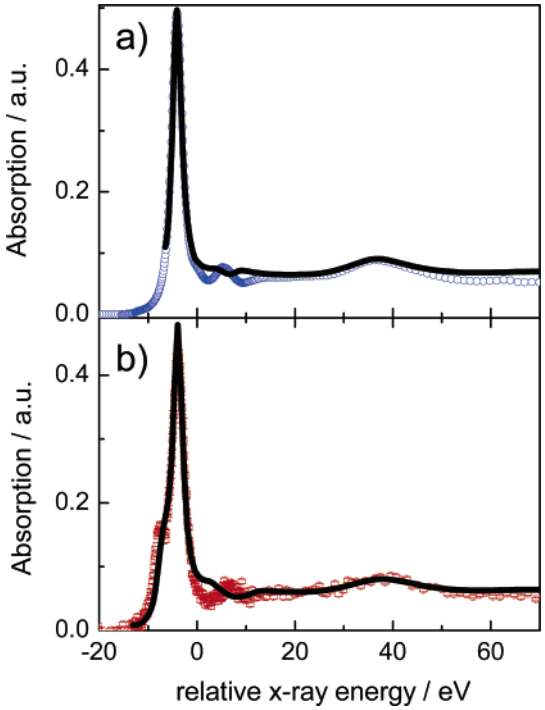

Figure 2. Fit using the muffin-tin (MT) approximation (back trace) of the ground (a) and excited (b) states experimental L_3-edge spectra (points) of aqueous $[Ru^{II}(bpy)_3]^{2+}$, taking a cluster of 37 atoms.

TABLE 1: Fit Parameters of the Full Spectra for the Ground and Excited States of the Complex[a]

	Ru−N_{up} (Å)	Ru−N_{down} (Å)	$\Delta\phi$	Γ_c (eV)	R_{sq}
ground state	2.06 (0.03)	2.06 (0.03)	1.91° (7°)	2.09	1.12
excited state	2.06 (0.04)	2.06 (0.04)	−7.89° (7.4°)	2.20	5.52

[a] Up (down) refers to the N atoms in the pyridine rings up (down) the plane perpendicular to the C_3 axis. $\Delta\phi$ represents the angle between one triplet of pyridines with respect to the other. Γ_c is the core hole lifetime and R_{sq} is the square residual function defined in the text.

Figure 2 shows the best fits for the ground- and excited-state experimental L_3-edge XAS spectra. The agreement is satisfactory over the entire energy region, apart for band C, that is missing in the calculation (this is discussed below), and the offset between simulated and experimental spectra at high energies. Nevertheless, for the ground state, the relatively good agreement confirms the quality of the method, given the available crystallographic data.[26,27] For the excited-state spectrum (Figure 2b), the calculation reproduces the new A′ band, although the A′−B′ energy splitting is smaller than in the experimental spectrum. This is due to a limitation of the MT approximation, which is less suitable for low-lying states.[14,28−30]

The fit results for both ground and excited states are given in Table 1. Within statistical error, the quality of fits is unable to retrieve a structural difference between the ground- and excited-state spectra.[16] In Table 1, we also report the value of the core hole lifetime coming from the Monte Carlo search in the nonstructural parameter space, and it is in good agreement with the literature value (the core hole lifetime of L_3 or Ru has been reported in the 1.7−2.0 eV range[31]). The main conclusion from Figure 2 and Table 1 is that fitting full spectra with MXAN is not sufficient to retrieve the subtle structural changes between ground and excited complex.

To identify the origin of band C, we performed several calculations using the FDM method. In this way, we can check the effect of the MT approximation. Figure 3 shows a comparison between the experimental excited-state spectrum and

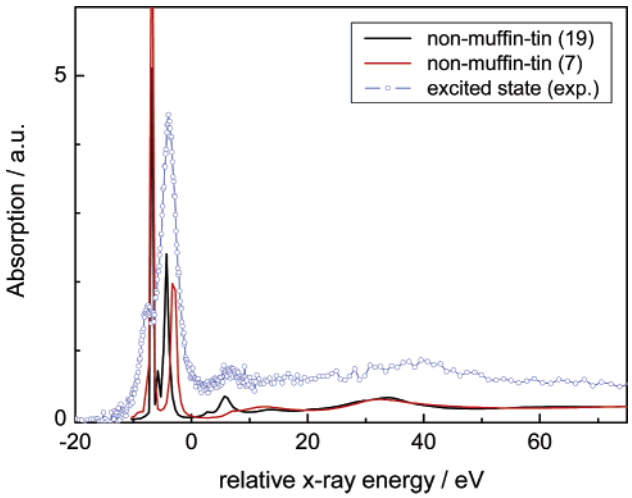

Figure 3. Non-MT calculations of the excited-state spectra for two clusters of 7 (red trace) and 19 (black trace) atoms, compared to the experimental spectrum (points).

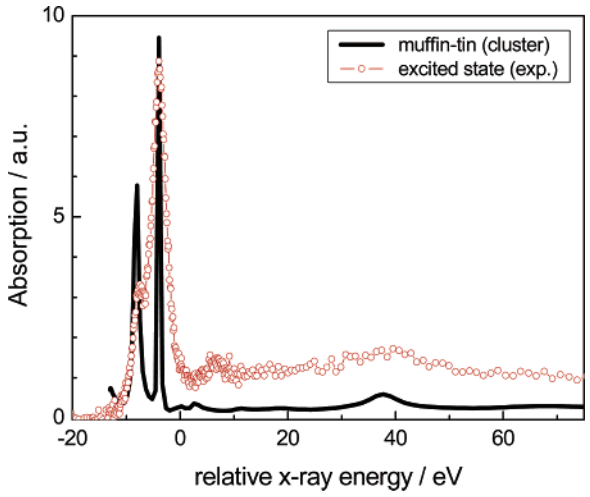

Figure 4. Simulation of the excited-state spectrum using MT without damping of the photoelectron wave, for a cluster of 37 atoms (i.e., the entire molecule, without the H atoms).

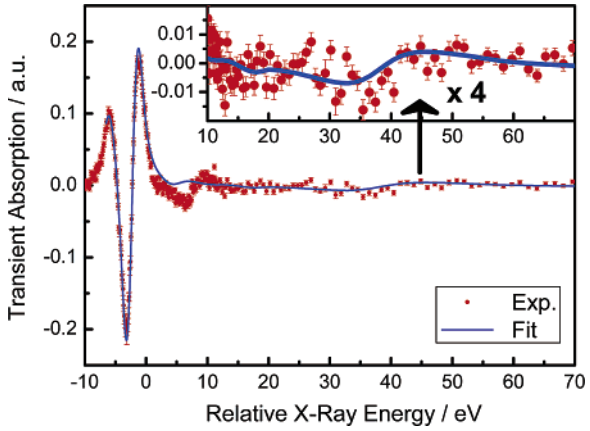

Figure 5. Fits of the difference XAS spectra using MT and a 37-atom cluster for a chemical shift of 1 eV. The inset shows a zoom of the D-band region.

two simulations, one using a small cluster of 7 atoms, i.e., only the neighboring nitrogen atoms around the absorber, and another one using the nearest 19 atoms (thus with 2 more carbon shells included). The theoretical calculations are made using only the real HL potential to put in evidence the effect of the cluster size. The computer time needed for this non-MT calculation makes it prohibitive to use a larger cluster, e.g., the entire molecule. However, the comparison between both sets gives insight into the overall trend. Peaks A′ and B′ are present in both calculations, confirming their bound−bound transition character, while peak C′ appears only when the cluster size is large enough to generate a multiple scattering (MS) resonance of sufficient amplitude. This confirms our previous tentative assignment[16] that band C is a true MS resonance, based on the fact that it lies 3.2 eV above the ionization limit, which corresponds to a photoelectron wavelength of ∼6.3 Å, i.e., on the order of the spatial extension of the molecule. It contradicts an earlier one,[32] which assigned band C to the 2p−5s bound−bound transition. Note also that the 19-atom case exhibits additional weak lines between the two main low-lying lines, compared to the 7-atom case, because the second shell of atoms provides an additional ligand field that is superimposed onto the main one, due to first-shell coordination.

We now return to the MT calculations, which allow a more detailed look into the geometric structural changes. In Figure 4, we show the comparison between the experimental data and the MT MXAN calculation performed using the entire 37-atom cluster and the real part of the HL potential. Peaks A′, B′, and D′ are located at the right relative energy position with a reasonable intensity ratio, while peak C′, though present, deviates strongly in intensity and energy position, because (discussed above) it is located in the energy range, where details of the potential can be important. Nevertheless, the non-MT corrections do not affect the extraction of structural information, because the later essentially involves the relative position of peaks B (B′) and D (D′) and their intensities, and because these corrections are essentially confined to the first 10 eV or so of the spectrum.

Since the fits of full spectra cannot reveal structural differences between the ground- and excited-state compounds, we fitted the difference spectra using the procedure described in section II. Figure 5 shows the fit taking the chemical shift of 1 eV determined in ref 16 and a core hole lifetime of 2.17 eV. Here, the sole adjustable structural parameter is the Ru−N distance. The result is satisfactory in the entire energy range, except in the region of band C, as expected. Note that the fit captures well, both in energy and in amplitude, the details of spectral changes in both the region of the edge (A,B-band region) and that of the D-band, well above (>20 eV) the edge. The latter is important, since the fit of the difference spectra is capable of capturing the small but noticeable spectral change at the D-band, which reflects a weak contraction of the Ru−N distance in the excited state. This clearly shows that fitting difference spectra is much more sensitive than fitting full spectra. In addition, the statistical quality of the fit is improved, as can be seen from the value of the square residual function R_{sq}= 1.89, to be compared with the value of 5.52 (Table 1) resulting from the fit of the full spectrum. Finally, the Ru−N bond contraction we obtain from the fit (0.045 Å) is in good agreement with the value derived in ref 16 (0.037 ± 0.0135 Å) using the FEFF8.2 code. As discussed then,[16] $[Ru^{II}(bpy)_3]^{2+}$ does not lend itself easily to a fit of the EXAFS features, as the energy range of the latter is rather limited (<130 eV). The present approach using MXAN does not suffer from this limitation, and it shows that the present fit under D_3 symmetry agrees with the results of ref 16.

As mentioned in the Introduction, from an electronic point of view, the system adopts a C_2 symmetry in the excited state, rather than a D_3 symmetry. Therefore, we also carried out fits of the difference spectra, assuming that two neutral bpy's remain

at fixed positions, while the Ru−N distance to the reduced bpy is used as an adjustable parameter. A reasonably good fit was obtained for a Ru−N bond contraction by ∼0.07 Å. However, given the quality of the data and the arbitrary assumptions (e.g., the two unmoved bpy ligands) made for this simulation, it is difficult to draw conclusions about the validity of the Ru−N bond contractions under one or the other symmetries. Nevertheless, this shows that MXAN can fit data reasonably well in the case of nontotally symmetric structural changes.

In conclusion, as far as $[Ru^{II}(bpy)_3]^{2+}$ is concerned, the present simulation allowed us to demonstrate the following: (i) that band C is a feature resulting from multiple scattering over the entire molecule, (ii) that the Ru−N bond contractions in the excited-state complex are in very good agreement with those derived in ref 16 when using a trigonal symmetry for the excited state, and (iii) that bond changes for nontotally symmetric distortions can be extracted from the fit.

On a more general perspective, the present methodology based on fitting difference absorption spectra introduces many novel advantages: (i) It increases the sensitivity and the statistical quality of the fit. In particular, the statistical error bars using transient difference spectra allow us to increase the sensitivity by a factor of ∼3 for the present data (based on the R_{sq} factors). (ii) There is no data reduction, as the fits are done in energy space, contrary to other methods where, e.g., Fourier transformation-related errors can occur due to truncation. (iii) The present work represents the first application of the MXAN code to L absorption edges. This point is of importance due to the role of transition-metal complexes in coordination chemistry and biology (protein binding sites). (iv) The methodology presented here is not limited to time-resolved light-induced difference spectra, but can be applied to any situation, where changes in XAS spectra are generated by temperature, pressure, pH, magnetic fields, and so forth.

Acknowledgment. This work was partly supported by the Swiss National Science Foundation via grants 620-066145 and 200021-105239/1, by the Swiss Light Source (Villigen), and by the DYNA program of the European Science Foundation.

References and Notes

(1) Bressler, C.; Chergui, M. *Chem. Rev.* **2004**, *104*, 1781−1812.
(2) Saes, M.; Bressler, C.; Abela, R.; Grolimund, D.; Johnson, S. L.; Heimann, P. A.; Chergui, M. *Phys. Rev. Lett.* **2003**, *90*, 047403−047401.
(3) Saes, M.; Bressler, C.; van Mourik, F.; Gawelda, W.; Kaiser, M.; Chergui, M.; Bressler, C.; Grolimund, D.; Abela, R.; Glover, T. E.; Heimann, P. A.; Schoenlein, R. W.; Johnson, S. L.; Lindenberg, A. M.; Falcone, R. W. *Rev. Sci. Instrum.* **2004**, *75*, 24−30.
(4) Saes, M. G. W.; Kaiser, M.; Tarnovsky, A.; Bressler, Ch.; Chergui, M.; Johnson, S. L.; Grolimund, D.; Abela, R. *Synchrotron Radiat. News* **2003**, *16*, 12.
(5) Gawelda, W.; Bressler, C.; Saes, M.; Kaiser, M.; Tarnovsky, A.; Grolimund, D.; Johnson, S. L.; Abela, R.; Chergui, M. *Phys. Scr.* **2005**, *T115*, 102.
(6) Pettifer, R. F.; Mathon, O.; Pascarelli, S.; Cooke, M. D.; Gibbs, M. R. J. *Nature (London)* **2005**, *435*, 78−81.
(7) Yokoyama, T.; Murakami, Y.; Kiguchi, M.; Komatsu, T.; Kojima, N. *Phys. Rev. B* **1998**, *58*, 14238−14244.
(8) Boca, R.; Vrbova, M.; Werner, R.; Haase, W. *Chem. Phys. Lett.* **2000**, *328*, 188−196.
(9) Baudelet, F.; Pascarelli, S.; Mathon, O.; Itie, J. P.; Polian, A.; d'Astuto, M.; Chervin, J. C. *J. Phys.: Condens. Matter* **2005**, *17*, S957−S966.
(10) Itie, J. P.; Baudelet, F.; Congeduti, A.; Couzinet, B.; Farges, F.; Polian, A. *J. Phys.: Condens. Matter* **2005**, *17*, S883−S888.
(11) Frank, P.; Carlson, R. M. K.; Carlson, E. J.; Hodgson, K. O. *Coord. Chem. Rev.* **2003**, *237*, 31−39.
(12) Flogeac, K.; Guillon, E.; Aplincourt, M. *Eur. J. Inorg. Chem.* **2005**, 1552−1558.
(13) Jezowska-Bojczuk, M.; Szczepanik, W.; Mangani, S.; Gaggelli, E.; Gaggelli, N.; Valensin, G. *Eur. J. Inorg. Chem.* **2005**, 3063−3071.
(14) Benfatto, M.; Congiu-Castellano, A.; Daniele, A.; Longa, S. D. *J Synchrotron Radiat.* **2001**, *8*, 267−269.
(15) Tyson, T. A.; Hodgson, K. O.; Natoli, C. R.; Benfatto, M. *Phys. Rev. B* **1992**, *46*, 5997−6019.
(16) Gawelda, W.; Johnson, M.; de Groot, F. M. F.; Abela, R.; Bressler, C.; Chergui, M. *J. Am. Chem. Soc.* **2006**, *128*, 5001−5009.
(17) Cannizzo, A.; van Mourik, F.; Gawelda, W.; Zgrablic, G.; Bressler, C.; Chergui, M. *Angew. Chem., Int. Ed.* **2006**, *45*, 3174−3176.
(18) de Groot, F. *Coord. Chem. Rev.* **2005**, *249*, 31−63.
(19) Benfatto, M.; D'Angelo, P.; Della Longa, S.; Pavel, N. V. *Phys. Rev. B* **2002**, *65*, 174205.
(20) Della Longa, S.; Arcovito, A.; Girasole, M.; Hazemann, J. L.; Benfatto, M. *Phys. Rev. Lett.* **2001**, *8715*, 155501.
(21) Benfatto, M.; Della Longa, S.; D'Angelo, P. *Phys. Scr.* **2005**, *T115*, 28.
(22) D'Angelo, P.; Benfatto, M.; Della Longa, S.; Pavel, N. V. *Phys. Rev. B* **2002**, *66*, 064209.
(23) Hayakawa, K.; Hatada, K.; D'Angelo, P.; Della Longa, S.; Natoli, C. R.; Benfatto, M. *J. Am. Chem. Soc.* **2004**, *126*, 15618−15623.
(24) Kimball, G. E.; Shortley, G. H. *Phys. Rev.* **1934**, *45*, 815.
(25) Joly, Y. *Phys. Rev. B* **2001**, *63*, article no. 125120.
(26) Rillema, D. P.; Jones, D. S.; Levy, H. A. *J. Chem. Soc., Chem. Comm.* **1979**, 849−851.
(27) Biner, M.; Bürgi, H. B.; Ludi, A.; Röhr, C. *J. Am. Chem. Soc.* **1992**, *114*, 5197−5203.
(28) Natoli, C. R.; Benfatto, M.; Doniach, S. *Phys. Rev. A* **1986**, *34*, 4682−4694.
(29) Foulis, D. L.; Pettifer, R. F.; Sherwood, P. *Europhys. Lett.* **1995**, *29*, 647−652.
(30) Cabaret, D.; Joly, Y.; Renevier, H.; Natoli, C. R. *J. Synchrotron Radiat.* **1999**, *6*, 258−260.
(31) Krause, M. O.; Oliver, J. H. *J. Phys. Chem. Ref. Data* **1979**, *8*, 329−338.
(32) Sham, T. K. *J. Am. Chem. Soc.* **1983**, *105*, 2269−2273.